AD-A071 284 IBM RESEARCH LAB SAN JOSE CALIF F/G 7/4
INTERFERENCE PULSES IN OPTICAL FREE INDUCTION DECAY,(U)
AUG 74 K L FOSTER, S STENHOLM, R G BREWER N00014-72-C-0153
UNCLASSIFIED RJ-1431 NL

END
DATE FILMED
8-79
DDC

IBM Research

INTERFERENCE PULSES IN OPTICAL FREE INDUCTION DECAY

K. L. Foster / S. Stenholm
Richard G. Brewer

August 16, 1974

RJ 1431

Yorktown Heights, New York
San Jose, California
Zurich, Switzerland

Limited Distribution Notice

This report has been submitted for publication elsewhere and has been issued as a Research Report for early dissemination of its contents. As a courtesy to the intended publisher, it should not be widely distributed until after the date of outside publication.

Copies may be requested from:
IBM Thomas J. Watson Research Center
Post Office Box 218
Yorktown Heights, New York 10598

AD A071284

DDC ACCESSION NUMBER

III

LEVEL

DATA SHEET

PHOTOGRAPH

THIS SHEET

1

INVENTORY

RJ-1431, Dtd. 16 Aug. '74
(#22101)

DOCUMENT IDENTIFICATION

DISTRIBUTION STATEMENT A
Approved for public release;
Distribution Unlimited

DISTRIBUTION STATEMENT

Accession For
NTIS GRA&I [X]
DDC TAB [ ]
Unannounced [ ]
Justification
Per FL-88 (R79-0951)
By on file
Distribution/
Availability Codes
Dist | Avail and/or special
A

DDC FILE COPY

DISTRIBUTION STAMP

DDC
RECEIVED
JUL 17 1979
D

DATE ACCESSIONED

79 06 29 057

DATE RECEIVED IN DDC

PHOTOGRAPH THIS COPY

RJ 1431 (#22101)
August 16, 1974
Physics (General)

INTERFERENCE PULSES IN OPTICAL FREE INDUCTION DECAY*

K. L. Foster
S. Stenholm†
Richard G. Brewer

IBM Research Laboratory
San Jose, California 95193

ABSTRACT: A new feature of optical free induction decay (FID) is observed in a coherently prepared sample of $^{13}CH_3F$ by the method of Stark switching. The preparative phase is due to the resonant steady state excitation by a cw laser beam and is followed by FID upon sudden application of a d.c. Stark field that switches the molecular sample out of resonance. The emission is not observed as a simple decay but instead appears as a train of sharp pulses regularly spaced in time due to a repetitive interference. This situation arises because an entire set of infrared transitions within the Stark split manifold are initially prepared, in contrast to our previous study of a nondegenerate transition. The emission, which beats with the laser, produces a heterodyne beat spectrum consisting of a set of regularly spaced frequencies that is the Fourier transform of the slowly decaying pulse progression observed. We thus demonstrate what is the optical analog of the well known NMR method of high resolution pulse Fourier spectroscopy. The detailed behavior of the pulse train agrees well with a FID theory that assumes the transitions to be uncoupled. The subtle behavior of FID near the time origin is explored also by approximate analytic expressions that reveal a near zero or a sizable amplitude depending on the degree of saturation in the preparative stage. The experimental technique discussed offers an attractive way for obtaining high resolution optical spectra without Doppler broadening and for generating an optical pulse train whose time scale can be compressed by simply increasing the Stark field.

---

*Work supported in part by the U.S. Office of Naval Research under Contract No. N00014-72-C-0153.

†On leave from the Research Institute for Theoretical Physics, University of Helsinki, 00170 Helsinki 17, Finland.

I. INTRODUCTION

In a previous article,[1] we reported the observation of optical free induction decay (FID). A molecular sample which is coherently prepared by a cw laser beam exhibits such a decay when it is suddenly switched out of resonance by a Stark field. In the case examined, a nondegenerate Doppler-broadened infrared transition of NH_2D displayed a simple decay behavior - the emission being coherent, intense, directional and of a single frequency. In this two level problem, FID produces a heterodyne beat signal at a detector because it and the laser beam are spatially coincident and are separated in frequency due to the Stark shift. Furthermore, the decay was rapid, being dominated by inhomogeneous dephasing due to the finite width of the velocity group affected by the steady state preparation.

It was presumed until recently that optical FID would show no unusual features when several transitions of a Stark multiplet are simultaneously prepared. Previous observations[2,3] in CH_3F have in fact yielded a simple decay devoid of any beat pattern because of the mutual interference of the many beat frequencies present.

We now find, however, that if the dephasing time is lengthened and other conditions satisfied, the FID interference shows a repetitive character, appearing as a series of sharp pulses or spikes as in Figure 1. This situation prevails when the Stark split spectrum consists of a set of regularly spaced lines. In first approximation, these results are explained by simple addition of the various Fourier components of the FID.

It will become evident that the time scale of the pulse train, i.e., the interval between pulses and the pulse width, are determined by the Stark field amplitude and the number of transitions.

The coherent phenomenon observed here superficially resembles mode locking in a laser in that several evenly spaced frequency components are involved. It differs, however, because in this case the regular frequency spacing is inherent in the transitions involved and no interaction between them is needed. Little evidence is, in fact, seen for a nonlinear coupling among the radiated waves.

II. FREE INDUCTION DECAY THEORY

We consider a set of overlapping optical transitions that are simultaneously excited in steady state by a laser field

$$E_x(z,t) = E_0 \cos(\Omega t - kz). \tag{1}$$

This prepares a coherent polarization in the medium, which exhibits FID when a step function Stark field is applied. The Stark field splits the transitions, which then emit a set of frequencies. We assume the various components to decay as uncoupled transitions, justifying the use of an analytical solution along the lines given by Brewer and Shoemaker[1] or Hopf et al.[4] for the two-level problem. When the emitted frequencies are equally spaced (see below) the observed signal displays a repetitive pulsing due to interference between the components. The uncoupled treatment satisfactorily explains most if not all features of the observed signals.

We first concentrate on one transition a-b with the energy difference $\hbar\omega_{ab}$. The 2×2 density matrix equation of motion

$$i\hbar\dot{\rho} = [H,\rho] + \text{relaxation terms} \tag{2}$$

gives for the quantities

$$\tilde{\rho}_{ab} \equiv \rho_{ab}\, e^{i(\Omega t - kz)} \tag{3}$$

$$\Delta\rho_{ba} \equiv \rho_{bb} - \rho_{aa} \tag{4}$$

the equations

$$\left[\frac{d}{dt} + i(\omega_{ab} - \Omega + kv) + \frac{1}{T_2}\right]\tilde{\rho}_{ab} = i\alpha\Delta\rho_{ba} \tag{5}$$

$$\frac{d}{dt}(\Delta\rho_{ba}) = 2i\alpha(\tilde{\rho}_{ab} - \tilde{\rho}_{ba}) - (\Delta\rho_{ba} - \Delta\rho_{ba}^{0})/T_1 \ . \tag{6}$$

Here, we have introduced

$$\alpha \equiv \frac{\mu_{ab}E_0}{2\hbar} \ ,$$

and $\Delta\rho_{ba}^{0}$ is the equilibrium value of $(\rho_{bb} - \rho_{aa})$ in the absence of the laser beam. Equation (5) contains the Doppler shift kv, and we introduce the longitudinal and transverse relaxation times T_1 and T_2 directly. This simplifies the treatment of Ref. 1 slightly.

During the steady state preparation, Eqs. (5) and (6) yield the solution

$$\tilde{\rho}_{ab}(0) = \frac{i\alpha[-i(\omega_{ab}-\Omega+kv) + 1/T_2]}{[(\omega_{ab}-\Omega+kv)^2 + 1/T_2^2 + 4\alpha^2 T_1/T_2]} \Delta\rho^0_{ba} \quad . \tag{7}$$

The corresponding steady state value for the population difference $\Delta\rho_{ba}(0)$ displays a similar saturation behavior.

When the Stark field is switched, the polarization given by (7) radiates at the new frequency $(\omega_{ab}+\Delta\omega_{ab})$. The time dependence is determined by Eq. (5) where, for not too long a time span, we can approximate $\Delta\rho_{ba}$ by its initial value. The solution for $t \geq 0$ is then

$$\tilde{\rho}_{ab}(t) = \tilde{\rho}_{ab}(0)\, e^{-[i(\omega_{ab}+\Delta\omega_{ab}-\Omega+kv) + 1/T_2]t}$$

$$+ i\alpha\Delta\rho_{ba}(0)\, \frac{1 - e^{-[i(\omega_{ab}+\Delta\omega_{ab}-\Omega+kv) + 1/T_2]t}}{i[\omega_{ab}+\Delta\omega_{ab}-\Omega+kv] + 1/T_2} \quad . \tag{8}$$

For the molecules nearly in resonance before switching, the second term is depressed by a factor $(\alpha/\Delta\omega_{ab})$ and hence is negligible; for molecules in resonance with the new transition frequency, this term provides the nutation signal. The FID signal derives entirely, therefore, from the first term of (8).

The polarization is given by

$$P_{ab} = N\mu_{ab} e^{-i(\Omega t - kz)} \langle \tilde{\rho}_{ab}(t) \rangle + c.c. \qquad (9)$$

where the Doppler averaged density matrix element is

$$\langle \tilde{\rho}_{ab}(t) \rangle = e^{-[i\Delta\omega_{ab} + 1/T_2]t}$$

$$\times \frac{1}{u\sqrt{\pi}} \int_{-\infty}^{+\infty} e^{-v^2/u^2} \frac{i\alpha[-i(\omega_{ab} - \Omega + kv) + 1/T_2] e^{-i(\omega_{ab} - \Omega + kv)t}}{[(\omega_{ab} - \Omega + kv)^2 + 1/T_2^2 + 4\alpha^2 T_1/T_2]} \Delta\rho_{ba}^0 \, dv$$

$$\approx \frac{i\alpha}{ku\sqrt{\pi}} \Delta\rho_{ba}^0 \, e^{-[i\Delta\omega_{ab} + 1/T_2]t} \, e^{-\left(\frac{\omega_{ab} - \Omega}{ku}\right)^2} \int_{-\infty}^{+\infty} \frac{[1/T_2 - ix] e^{-ixt}}{[x^2 + 1/T_2^2 + 4\alpha^2 T_1/T_2]} \, dx \, .$$

(10)

Here we assume that the Doppler factor can be taken outside the integral; this approach neglects some features of the experiment which we will discuss in the Appendix. Because $t > 0$, the integration path can be closed in the lower complex half-plane with one single pole at $x = -i/T_2[1 + 4\alpha^2 T_1 T_2]^{1/2}$ giving the result

$$\langle \tilde{\rho}_{ab}(t) \rangle = - \frac{i\alpha\sqrt{\pi}\Delta\rho_{ba}^0}{ku} \left[1 - \frac{1}{\sqrt{1 + 4\alpha^2 T_1 T_2}} \right] e^{-i\Delta\omega_{ab} t} \, e^{-(\omega_{ab} - \Omega)^2 / k^2 u^2}$$

$$\times \exp\left[-(1 + \sqrt{1 + 4\alpha^2 T_1 T_2}) t/T_2 \right] \, . \qquad (11)$$

The polarization (9) induces the signal field

$$E_s(z,t) = E_{ab}(z,t)e^{-i(\Omega t-kz)} + c.c. \tag{12}$$

which can be calculated from Maxwell's equations in the form

$$\frac{\partial E_{ab}}{\partial z} = 2\pi ikN\mu_{ab}\langle\tilde{\rho}_{ab}\rangle . \tag{13}$$

Assuming the z integration to contribute the optical path length L as a factor, we get from (13) and (11) the result

$$E_{ab} = Q_{ab}(t)e^{-i[(\Omega+\Delta\omega_{ab})t - kz]} \tag{14}$$

where the prefactor

$$Q_{ab}(t) = \frac{\pi^{3/2}\, NL\mu_{ab}^2 E_0 \Delta\rho_{ba}^0}{u\hbar}\left[1 - \frac{1}{\sqrt{1 + 4\alpha^2 T_1 T_2}}\right] e^{-(\omega_{ab}-\Omega)^2/k^2u^2}$$

$$\times \exp\left[-(1+\sqrt{1+4\alpha^2 T_1 T_2})t/T_2\right] . \tag{15}$$

For one transition, the result (14)-(15) agree with those of Refs. 1 and 4.

The total field striking the detector is (12) plus (1) and the heterodyne beat signal is given by the cross product

$$(E^2)_{beat} = \frac{1}{2} \sum_{[ab]} E_0 Q_{ab}(t) e^{-i\Delta\omega_{ab}t} + c.c.$$

$$= \sum_{[ab]} E_0 Q_{ab}(t) \cos \Delta\omega_{ab} t \qquad (16)$$

where [ab] indicates the sum over the signals from all transitions affected by the steady state preparation.

It now remains to complete the summation of (16). The experiment to be discussed involves a ν_3 band vibration-rotation infrared transition of CH_3F where (J,K) = (5,3) → (4,3) and the upper (5,3) and lower (4,3) levels exhibit a first order Stark splitting[5,6] in the presence of a static electric field ε

$$\Delta W_1 = - \frac{\mu \varepsilon M K}{J(J+1)} \quad . \qquad (17)$$

The optical selection rule of interest, among the space quantized states, is ΔM = 0 so that the change in transition frequency $\Delta\omega_{ba}$ due to the step function Stark field is

$$\Delta\omega_{ba} = \frac{1}{\hbar} \left[\frac{\mu' K}{J'(J'+1)} - \frac{\mu'' K}{J''(J''+1)} \right] M\varepsilon = \delta M \varepsilon$$

$$\delta \equiv \frac{1}{\hbar} \left[\frac{\mu' K}{J'(J'+1)} - \frac{\mu'' K}{J''(J''+1)} \right] . \qquad (18)$$

This is the quantity appearing in (16) where M = -4, -3...3, 4. The permanent electric dipole moment[5] μ and the rotational quantum numbers J

and K are labeled by single and double primes as they pertain to upper or lower transition levels. The optical or beat spectrum, therefore, consists of a series of 9 lines, regularly spaced with a frequency interval $\delta\varepsilon$ as shown in Figure 2.

Note that the transition strength in Q_{ba} is given by $\mu_{ba}^2 \propto (J'^2-M^2)$ where $J' = 5$ in this case and Eq. (16) may be evaluated numerically using (18). We assume for simplicity that the Stark bias field is zero making the Doppler factors $\exp[-(\omega_{ab}-\Omega)^2/k^2u^2]$ all equal, and we omit damping. The result of such a calculation is given in Figure 3 and shows the repetitive interference or pulsing phenomenon - a series of prominent sharp pulses.

More insight can be obtained, however, by letting all line strengths be equal. Equation (16) then becomes

$$(E^2)_{beat} = E_0Q \sum_{M=-4}^{+4} \cos(\delta M\varepsilon t) = E_0Q \frac{\sin(9\delta\varepsilon t/2)}{\sin(\delta\varepsilon t/2)} . \qquad (19)$$

This shows that pulses occur at regular intervals T given by

$$T = \frac{2\pi}{\delta\varepsilon} . \qquad (20)$$

An approximate value for the pulse width can be found from the zero of the numerator of (19) or $\Delta T = \frac{2\pi}{9\delta\varepsilon} = T/9$ so that the pulse interval to width ratio is $T/\Delta T = 9$, i.e., just the number of transitions involved. The more accurate value deduced from Figure 3 yields

$$T/\Delta T = 6.25 \tag{21}$$

where ΔT is the FWHM value. The time scale becomes compressed as either the number of transitions, the Stark tuning rate δ or the Stark field ε increases.

If the optical selection rule is not $\Delta M = 0$ but rather $\Delta M = \pm 1$, similar arguments lead to

$$(E^2)_{beat} = 2E_0 Q \cos(\Delta_u \varepsilon t)\, \frac{\sin(9\delta\varepsilon t/2)}{\sin(\delta\varepsilon t/2)} , \tag{22}$$

when in (16) we introduce

$$\Delta\omega_{ba} = \frac{1}{\hbar}\left[\frac{\mu' K(M\pm 1)}{J'(J'+1)} - \frac{\mu'' KM}{J''(J''+1)}\right]\varepsilon \equiv (\delta M \pm \Delta_u)\varepsilon ,$$

$$\Delta_u = \frac{1}{\hbar}\left[\frac{\mu' K}{J'(J'+1)}\right] . \tag{23}$$

The behavior of (22) has the same characteristic pulse interval and width as (19), but in addition, it is modulated by $\cos\Delta_u \varepsilon t$ which interestingly causes some of the pulses to be positive and others negative.

III. THE EXPERIMENT

The Stark switching technique[1-3] and the experimental design for monitoring optical coherent transients has been described previously and does not require extensive elaboration here. A cw CO_2 laser beam of ~1 W

traverses an optical Stark cell containing a low pressure gas (~100μTorr), a sample of $^{13}CH_3F$, before striking a germanium-gold doped detector. Transient signals are stored in a Princeton Applied Research Box Car Integrator (PAR160) before being displayed on an X-Y recorder. The P(32) CO_2 line at 1035.474 cm^{-1} is utilized as it conveniently falls within the 66 MHz Doppler width of the ν_3 band line (J,K) = (4,3) ↔ (5,3) of $^{13}CH_3F$, which is 90% enriched.

The principal modification in the apparatus is the use of a large optical Stark cell having a 2 inch gap spacing and an optical path length of 18 inches. By means of a Galilean telescope, the laser beam is expanded from ~0.1 inch to 2 inch diameter to match the transverse cell dimension. The longer path length affords a higher sensitivity and thus a lower gas pressure than the smaller cells previously used, thereby reducing the dephasing from molecular collisions. The increased laser beam diameter, on the other hand, reduces the inhomogeneous dephasing expressed in (15) ($\alpha = \mu_{ab}E_0/2\hbar$ is smaller). The FID signals thus persist about one order of magnitude longer in time than in previous studies, i.e., for about 7μsec. It is primarily for these reasons that the repetitive interference pulses can be so clearly seen.

Figure 1 illustrates the FID pulse train for $\Delta M = 0$ selection rules, and Figure 2 gives the observed beat spectrum for the same experimental conditions with the predicted 9 line spectrum underneath. The observed pulse interval T = 860 nsec agrees well with the observed beat interval 1.166 MHz (858 nsec), but differs slightly from the calculated value 890 nsec

based on Eq. (18), probably due to an uncertainty in the Stark field measurement. For this run, the pressure was 100 μTorr and the Stark field 130 V/cm.

The pulse width in Figure 1 is found to be ΔT = 150 nsec so that $T/\Delta T$ = 5.7, which departs slightly from $T/\Delta T$ = 6.25 predicted in (21). Since the photodetector's rise and fall time can contribute ~30 nsec to the total pulse width, the pulses are certainly narrower and a more accurate measurement would approach the prediction even more closely.

The beat spectrum of Figure 2, it will be noticed, contains at least 8 weak beats in addition to the predicted 9 line spectrum. We believe that these additional beats are an artifact produced by electronic nonlinearities rather than by optical polarization nonlinearities. A numerical Fourier transform of Figure 2(a) does not agree accurately with Figure 1 as it should, and in fact, does not reproduce the weak triplet of pulses lying between two principal pulses. Optical nonlinearities also appear unlikely for the reason that the FID intensity is only ~1 μW.

On the other hand, a numerical Fourier transform of Figure 2(b) or Eq. (16) results in the pulse train of Figure 3. The first three main pulses are shown where damping and the finite spectral width of each beat have been neglected. We now see that the triplet structure emerges in agreement with Figure 1; the triplet is a consequence of the sin $(9\delta\epsilon t/2)$ term of Eq. (19) which performs 8 zero crossings between two large pulses.

The close correspondence between Figures 1 and 3 in this respect is strong confirmation that the model of uncoupled transitions closely represents the observations.

Experiments with $\Delta M = \pm 1$ selection rules give more complex pulse trains than Figure 1 where some pulses show positive and others negative excursions in conformity with (22). We have not studied this case in any detail as the signals are weaker than the $\Delta M = 0$ case.

It is tempting to consider the use of higher Stark fields that would have the effect of compressing the time scale of the experiment. Rather modest fields of ~130 V/cm have been applied here but it should be possible to achieve ~100,000 V/cm corresponding to ~100 psec infrared pulses. In addition, this is the optical analog of the fast Fourier transform pulse technique that has been so successfully used in high resolution NMR spectra.

ACKNOWLEDGMENT

We are indebted to R. L. Shoemaker, F. Shimizu, M. Sargent and E. L. Hahn for clarifying discussions.

REFERENCES

1. R. G. Brewer and R. L. Shoemaker, Phys. Rev. A6, 2001 (1972).

2. R. G. Brewer and R. L. Shoemaker, Phys. Rev. Letters 27, 631 (1971).

3. R. L. Shoemaker and R. G. Brewer, Phys. Rev. Letters 28, 1430 (1972).

4. F. A. Hopf, R. F. Shea and M. O. Scully, Phys. Rev. A7, 2105 (1973).

5. R. L. Shoemaker, S. Stenholm and R. G. Brewer (to be published). Here $\mu' = 1.9038(6)$ debye and $\mu'' = 1.8578(6)$ debye.

6. C. H. Townes and A. L. Schawlow, Microwave Spectroscopy (McGraw-Hill, New York, 1955), p. 256.

7. P. F. Liao and S. R. Hartmann, Physics Letters 44A, 361 (1973).

8. A. G. Anderson and S. R. Hartmann, Phys. Rev. 128, 2023 (1962), see e.g., Eqs. (44) and (110).

APPENDIX

Here we consider some of the details of the evaluation of the FID signal Eq. (11). The calculations show that the signal for short times depends on the details of the velocity distribution in a more subtle way than the straightforward evaluation in the text. This clarifies an apparent discrepancy between the work by Liao and Hartmann[7] and the simple exponental decay used here and previously derived in Refs. 1 and 4.

The integral to be calculated in (10) is of the form

$$\int_{-\infty}^{+\infty} \frac{\gamma - ix}{x^2+\Gamma^2}\; e^{-ixt}\; e^{-(x-\Delta)^2/\sigma^2}\; dx = \frac{\gamma}{\Gamma} A(t) - B(t) \qquad (A.1)$$

where $\gamma = T_2^{-1}$, $\Gamma^2 = T_2^{-2} + 4\alpha^2 T_1/T_2$, $\Delta = \Omega - \omega_{ab}$ and $\sigma = ku$. We separate the integral into two parts: the A part containing the Lorentzian $\Gamma/(x^2+\Gamma^2)$ and the B part, the dispersion $ix/(x^2+\Gamma^2)$. In Eq. (10) we have set $x = 0$ in the Gaussian on account of the fact that

$$\Gamma \ll \sigma \; . \qquad (A.2)$$

We wish to consider this approximation in some detail.

The exact relation

$$B(t) = -\frac{1}{\Gamma}\frac{dA(t)}{dt} \; , \qquad (A.3)$$

can easily be proven and it suffices to evaluate A(t). When only A(t) is needed, the inequality (A.2) justifies the removal of the Gaussian from the integral, but for B(t) this is a moot point. Namely, for small t the B integral becomes logarithmically divergent at infinity and only converges thanks to the rapid oscillations of the exponential for large x. Thus, some care is needed when the limit t = 0 is taken.

We can transform the integral

$$A(t) = \int_{-\infty}^{+\infty} \frac{\Gamma}{(x^2+\Gamma^2)} \, e^{-itx} \, e^{-(x-\Delta)^2/\sigma^2} \, dx \tag{A.4}$$

by writing

$$\frac{\Gamma}{(x^2+\Gamma^2)} = \frac{1}{2} \int_{-\infty}^{+\infty} e^{ixs} \, e^{-\Gamma|s|} \, ds \tag{A.5}$$

$$e^{-(x-\Delta)^2/\sigma^2} = \frac{\sigma}{2\sqrt{\pi}} \int_{-\infty}^{+\infty} e^{i(x-\Delta)r} \, e^{-\frac{1}{4}\sigma^2 r^2} \, dr \tag{A.6}$$

and performing the r-integral by

$$\int_{-\infty}^{+\infty} e^{i(s-t+r)x} \, dx = 2\pi\delta(s-t+r) \, . \tag{A.7}$$

We obtain

$$A(t) = \pi\left(\frac{\sigma}{2\sqrt{\pi}}\right)\int_{-\infty}^{+\infty} e^{-\Gamma|s|}\, e^{-i\Delta(t-s)}\, e^{-\frac{1}{4}\sigma^2(t-s)^2}\, ds$$

$$= \pi\left(\frac{\sigma}{2\sqrt{\pi}}\right)\int_0^{\infty} ds\, e^{-\Gamma s}\left[e^{-i\Delta(t-s)}\, e^{-\frac{\sigma^2}{4}(t-s)^2} + e^{-i\Delta(t+s)}\, e^{-\frac{\sigma^2}{4}(t+s)^2}\right]. \tag{A.8}$$

For $\sigma >> \Gamma,\Delta$ and $t > \sigma^{-1}$ we can replace the Gaussian by a delta function

$$\frac{\sigma}{2\sqrt{\pi}}\, e^{-\frac{\sigma^2}{4}x^2} = \delta(x) \tag{A.9}$$

and (A.8) gives

$$A(t) = \pi e^{-\Gamma t} \tag{A.10}$$

At $t = 0$, (A.8) is exactly

$$A(0) = \pi\left(\frac{\sigma}{2\sqrt{\pi}}\right)\int_0^{\infty} e^{-\Gamma s}\, e^{-\frac{\sigma^2}{4}s^2}\, 2\cos\Delta s\, ds\ . \tag{A.11}$$

When $\Delta = 0$, this is easily seen to give $A(0) = \pi$ in the limit (A.2), which shows that the approximation (A.10) is valid also for small values of t.

To obtain B(t) we apply (A.3) to (A.8) and find that

$$B(t) = -\frac{1}{\Gamma}\left\{\pi\left(\frac{\sigma}{2\sqrt{\pi}}\right)\int_0^\infty ds\, e^{-\Gamma s}\,\frac{d}{dt}\left[-e^{-i\Delta(t-s)}\, e^{-\frac{\sigma^2}{4}(t-s)^2} + e^{-i\Delta(t+s)}\, e^{-\frac{\sigma^2}{4}(t+s)^2}\right]\right\}$$

$$= -\frac{1}{\Gamma}\left\{\pi\left(\frac{\sigma}{2\sqrt{\pi}}\right)\int_0^\infty ds\, e^{-\Gamma s}\,\frac{d}{ds}\left[-e^{-i\Delta(t-s)}\, e^{-\frac{\sigma^2}{4}(t-s)^2} + e^{-i\Delta(t+s)}\, e^{-\frac{\sigma^2}{4}(t+s)^2}\right]\right\}$$

$$= \pi\left(\frac{\sigma}{2\sqrt{\pi}}\right)\int_0^\infty ds\, e^{-\Gamma s}\left[e^{-i\Delta(t-s)}\, e^{-\frac{\sigma^2}{4}(t-s)^2} - e^{-i\Delta(t+s)}\, e^{-\frac{\sigma^2}{4}(t+s)^2}\right], \tag{A.12}$$

where the last result is obtained by an integration by parts. Note the simple relation between (A.8) and (A.12).

For large times we can again use the limit (A.9) and obtain

$$B(t) = \pi\, e^{-\Gamma t} \tag{A.13}$$

which approximation is consistent with (A.10) through (A.3). The observed signal (A.1) is written

$$\frac{\gamma}{\Gamma} A(t) - B(t) = \pi\, e^{-\Gamma t}\left[\frac{1}{\sqrt{1+4\alpha^2 T_1 T_2}} - 1\right] \tag{A.14}$$

which shows the validity of the result (11) in the main text for times $t > \sigma^{-1} << \Gamma^{-1}$.

For $t \lesssim \sigma^{-1}$, the behavior of B(t) does, however, differ from (A.13). At t = 0 we obtain from (A.12) the exact result

$$B(0) = \pi \left(\frac{\sigma}{2\sqrt{\pi}} \right) \int_0^\infty e^{-\Gamma s} e^{-\frac{\sigma^2 s^2}{4}} (2i \sin \Delta s)\, ds \qquad (A.15)$$

which is seen to vanish for resonant tuning $\Delta = 0$. Consequently, B(t) starts from zero and approaches the behavior (A.13) only after a time span of the order of σ^{-1}. On the other hand A(t) is described by (A.10) for all times.

At the initial time only A(t) is observed, but going back to (A.1), we can see that its contribution is suppressed by the factor

$$\frac{\gamma}{\Gamma} = \frac{1}{\sqrt{1+4\alpha^2 T_1 T_2}} < 1 \ . \qquad (A.16)$$

For an intense optical field, the molecular system is strongly saturated during the preparation and this factor becomes very small. We then expect the FID signal to start from a value near zero and increase to a maximum after a time σ^{-1} and subsequently decay as in Eq. (11). On the other hand, for $\gamma \lesssim \Gamma$ the FID signal has a large initial value due to the A term while B is still zero, and changes sign within a time of order σ^{-1} and approaches the behavior (A.14).

For the CH_3F experiment, the parameters are $\gamma \lesssim \Gamma \approx 10^5$ Hz and $\sigma = 66$ MHz. Hence (γ/Γ) is of the order $\frac{1}{2}$ and A(t) is expected to give a sizable contribution at t = 0. The experiments of Ref. 1 show the simple exponential decay of (11) to dominate the long time behavior but the short time behavior $\sim\sigma^{-1} \sim 10$ ns has not been experimentally resolved yet.

Liao and Hartmann[7] suggest an initial zero in the optical FID signal in ruby on account of the observation of a notched photon echo. Their experiment presumably takes place in the regime where the B component dominates.

For resonant tuning $\Delta = 0$ and short times, we expand the integral (A.12) in a power series in time. We can see that only odd terms contribute and

$$B(t) = \pi\left(\frac{\sigma}{2\sqrt{\pi}}\right)\int_0^\infty ds\left(e^{-\Gamma s}\, e^{-\frac{\sigma^2 s^2}{4}}\, \sigma^2 st\right) + O(t^3)$$

$$\approx \sqrt{\pi}\sigma t + O(t^3), \qquad \text{(A.17)}$$

where the limit (A.2) is used.

The Eq. (A.17) again shows that B(0) = 0, and gives a behavior which for short times agrees with that found by Anderson and Hartmann[8] for spin resonance. Their result is obtained when the Lorentzian is omitted from (A.4), in which case the integration is simple and (A.3) shows that

$B(t) \propto t \exp(-\text{const. } t^2)$. For times of the order Γ^{-1} the Lorentzian becomes essential and their result differs from the presently found behavior (A.14) leading to Eq. (11) of the text.

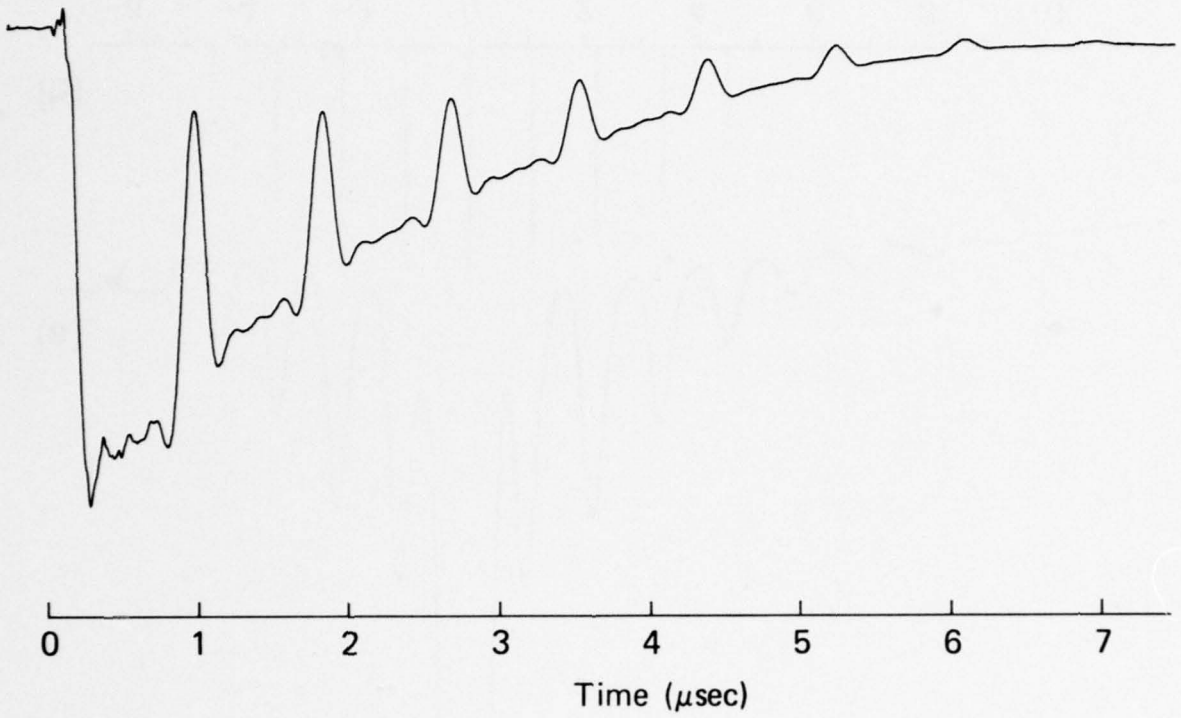

Figure 1. Free induction decay pulses observed in $^{13}CH_3F$.

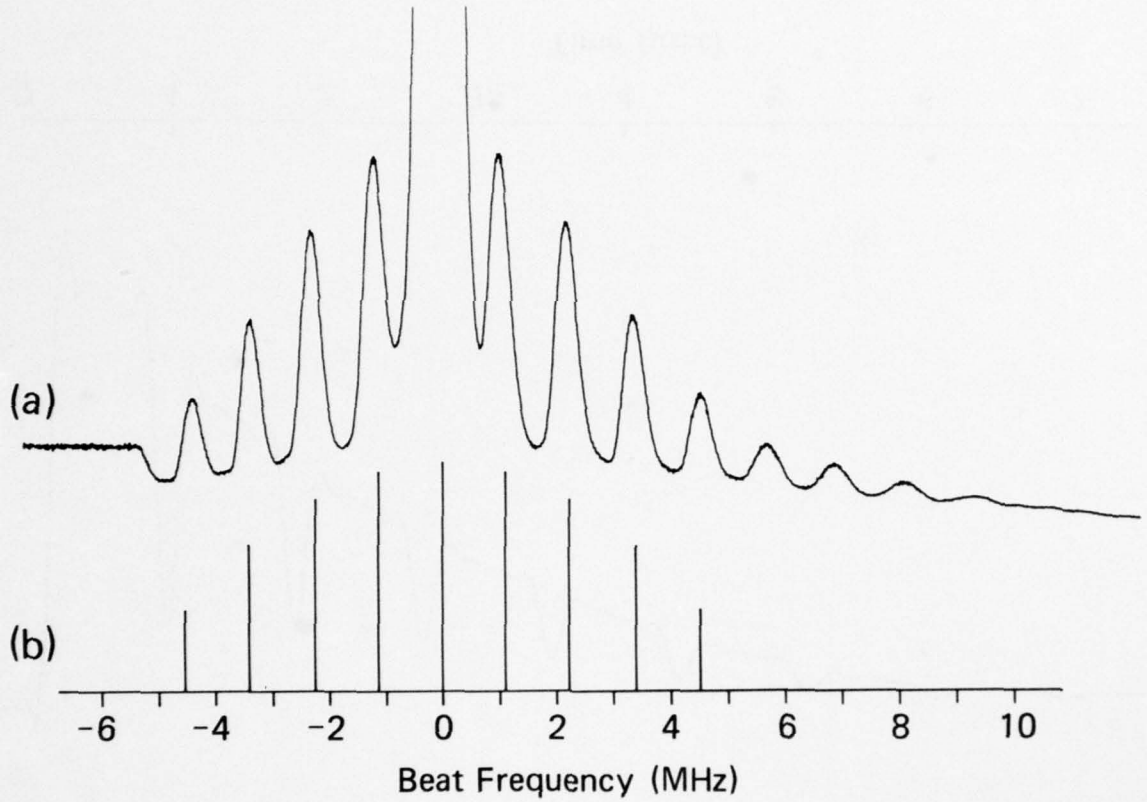

Figure 2. Heterodyne beat spectrum of $^{13}CH_3F$ free induction decay. The experimental conditions are the same as in Figure 1. A Hewlett-Packard 8553B Spectrum Analyzer was used. (a) Observed spectrum. (b) Predicted spectrum. The vertical scales are linear. In (a), beats are not seen below -5 MHz due to instru instrumental limitations.

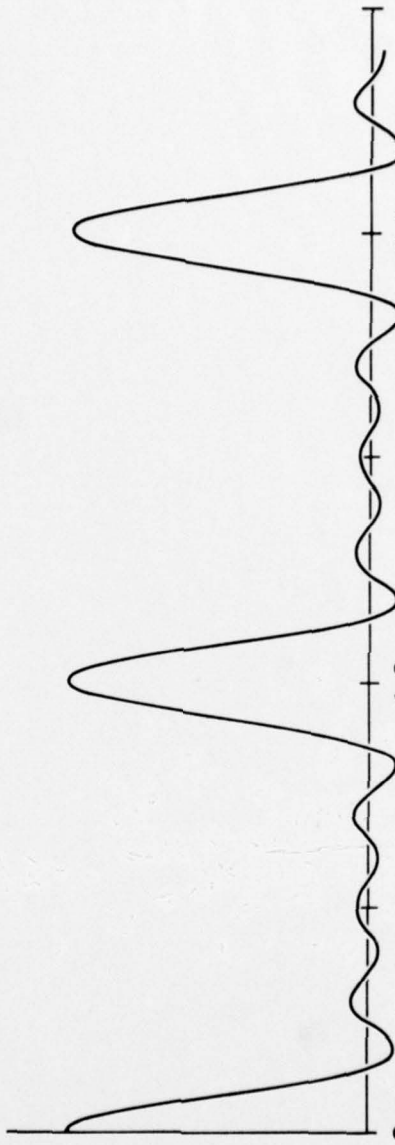

Figure 3. Free induction decay pulses calculated from Eq. (16) where the x axis is in normalized time units $\delta \epsilon t/2\pi$.